Unsteady Flow Calculation Using Implicit Method on a Moving Grid

Hiromasa Hayashi

Abstract

Today, much attention is devoted to unsteady flow problem such as flutter, for which flutter analysis with numerical simulation is useful in predicting conditions under which flutter occurs. To compute such a problem, this study specifically examines Moving Grid Finite Volume Method (FVM). Unsteady flow calculation code was constructed based on Moving Grid FVM. Then, the flow the field around an ONERA M6 wing was computed, which is a steady problem. Computational results show good agreement with experimental values on the undersurface of the wing. However, some gaps occurred between them near the shock above the wing. Lastly, a pitching problem of the NACA 0012 wing, which is an unsteady problem, was computed. The trend of computational results agrees with the experimental one. However, some gaps between these are apparent. Viscosity must be considered for accurate computation. Future work will include consideration of Navier–Stokes equations, performance of flutter simulation, and application of an unstructured grid to calculate the flow field around complicated objects.

1. Introduction

1.1 Development of Airplane and flutter

In airplane development, unsteady flow problems such as flutter that the unsteady nature has an extremely important sense have attracted attention. Flutter is a representative example of an aeroelastic phenomenon that occurs by an aerodynamic force and elastic force. A steady aerodynamic force, an elastic restoring force and unsteady aerodynamic force which depends on structural deformation work on a wing when a flight condition surpasses the flutter boundary. Divergence vibration of a wing by the force is called as flutter. Especially during high-speed flight, it might cause wing destruction by aerodynamic forces which amplify the vibration. Therefore flutter is a very important phenomenon in airplane design. Presently, various novel ideas including the use of composite materials such as carbon fiber reinforced plastic (CFRP) for airplanes are being explored to shorten flight times and to improve fuel efficiency. However, flutter characteristic degrades by stiffness decrease when weight saving of airplanes is performed. Therefore, it is necessary to predict the flutter boundary and avert the condition where flutter occurs for the safe design and operation of an airplane. To do this, an accurate prediction of the flutter boundary which used numerical calculation is expected.

1.2 Flutter analysis

It is necessary to combine Computational Fluid Dynamics (CFD) and structural calculation when flutter is reproduced with numerical simulation. In flutter analysis, a pressure distribution obtained by CFD is provided to structural calculation. Structural calculation is done with the distribution and displacement of a wing surface is computed. After spatial grid is deformed based on the displacement, CFD is performed. Fluid-Structure Interaction (FSI) calculation is done by repeating this cycle. Here, it is necessary to devote attention to discretization of the governing equations, evaluation of metrics, and so on in CFD because the grid moves in response to the translation and the deformation of a wing. The conservation law of the flow is not satisfied and the numerical calculation is not done accurately if the discretization and evaluation are made without careful consideration. To resolve this problem, the geometry conservation law (GCL) must be fulfilled, coupled with the conservation law of flow. In the conventional method [1], the GCL is discretized and solved in common with fluid conservation law. However, it is impossible to lead the error of metrics to zero in this method. Therefore, the Moving Grid Finite Volume Method (FVM) [2] is examined specifically, in which the control volume is extended in time and space. By applying this method, the GCL is absolutely satisfied.

1.3 Objective

The objective of this work is to construct an unsteady flow calculation code and perform flutter analysis. First, Moving Grid FVM is formulated. Secondly, the flow field around an ONERA M6 wing, which is a steady problem, is computed. Lastly, the pitching problem of the NACA 0012 wing, which is an unsteady problem, is computed. When these calculations are completed, the structured grid is used.

2. Numerical Calculation Methods

2.1 Moving Grid FVM

For ease of calculation, Euler equations are solved and viscosity is ignored. As stated in the *Introduction*, three-dimensional Euler equations are integrated in time and space based on Moving Grid FVM. Then the following are derived:

$$\int\int\int\int_{\Omega}\left(\frac{\partial \mathbf{Q}}{\partial t}+\frac{\partial \mathbf{E}}{\partial x}+\frac{\partial \mathbf{F}}{\partial y}+\frac{\partial \mathbf{G}}{\partial z}\right)\mathrm{d}\Omega = 0.$$

The Ω shows the control volume on time and space, with **Q**, **E**, **F**, and **G** shown as follows.

$$\mathbf{Q}=\begin{bmatrix}\rho\\ \rho u\\ \rho v\\ \rho w\\ e\end{bmatrix},\mathbf{E}=\begin{bmatrix}\rho u\\ \rho u^2+p\\ \rho uv\\ \rho uw\\ (e+p)u\end{bmatrix},\mathbf{F}=\begin{bmatrix}\rho v\\ \rho uv\\ \rho v^2+p\\ \rho vw\\ (e+p)v\end{bmatrix},\mathbf{G}=\begin{bmatrix}\rho w\\ \rho uw\\ \rho vw\\ \rho w^2+p\\ (e+p)w\end{bmatrix}.$$

After applying the divergence theorem of Gauss to the upper equations, the equations below are derived.

$$\mathbf{Q}^{\mathrm{n}+1}V_8-\mathbf{Q}^{\mathrm{n}}V_7+\sum_{k=1}^{6}\left(\mathbf{Q}^{n+\frac{1}{2}}n_t+\mathbf{E}^{\mathrm{n}+\frac{1}{2}}n_x+\mathbf{F}^{n+\frac{1}{2}}n_y+\mathbf{G}^{n+\frac{1}{2}}n_z\right)_k V_k=\mathbf{0}. \cdot\cdot\cdot (1)$$

Figure 1 presents a schematic of Moving Grid FVM. Black lines are at the *n* step, red lines are at the

n+1 step, and blue dashed lines are the locus of grid points. k=1–6 shows a hexahedral element shaped by a face at the n step and a face at the n+1 step. k=7 shows a hexahedral element formed by black lines at the n step. k=8 shows a hexahedral element that consists of red lines at the n+1 step. Here, the superscript shows the time step; n_t, n_x, n_y and n_z are components of a normal vector about a hexahedral element at k. Therefore, quantities at the $n+\frac{1}{2}$ step are evaluated on the average of quantities at the n step and at the n+1 step. By taking an average in this way, the time accuracy becomes second accuracy. In this method, these equations are an implicit form. Then, **E**, **F** and **G** are linearized and useful equations are obtained as shown below.

$$\left\{\mathbf{I}+\frac{1}{2V_8}\sum_{k=1}^{6}\left(\mathbf{I}n_t+\mathbf{A}n_x+\mathbf{B}n_y+\mathbf{C}n_z\right)_k^n V_k\right\}\Delta\mathbf{Q}^n$$
$$=-\frac{1}{V_8}\left\{\mathbf{Q}^n V_8-\mathbf{Q}^n V_7+\sum_{k=1}^{6}\left(\mathbf{Q}n_t+\mathbf{E}n_x+\mathbf{F}n_y+\mathbf{G}n_z\right)_k^n V_k\right\}.$$

There, **A**, **B**, and **C** show the Jacobian of **E**, **F** and **G**; $\Delta\mathbf{Q}^n$ is equal to $\mathbf{Q}^{n+1}-\mathbf{Q}^n$. The upper equations are formulated using Moving Grid FVM.

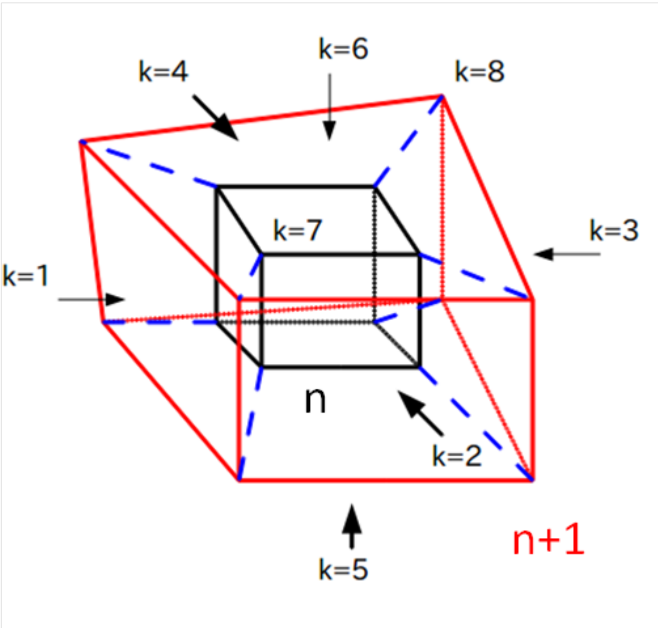

Fig. 1 Schematic of Moving Grid FVM.

2.2 Inner Iteration Method

To calculate unsteady flow problems, it is necessary to devote attention to time accuracy. If the equations described previously are solved as they are, then the temporal accuracy decreases because of the error of linearization, diagonalization, and approximate factorization. Therefore, the inner iteration method, designated as the delta form, is introduced into the equations to maintain temporal precision. The delta form is represented as

$$\mathbf{Q}^{n+1}=\mathbf{Q}^{(m)}+\Delta\mathbf{Q}^{(m)}.$$

Superscript *m* denotes the number of inner iterations. The equations to which delta form is applied are the following.

$$\left\{\mathbf{I}+\frac{1}{2V_8}\sum_{k=1}^{6}\left(\mathbf{I}n_t+\mathbf{A}n_x+\mathbf{B}n_y+\mathbf{C}n_z\right)_k^{(m)}V_k\right\}\Delta\mathbf{Q}^{(m)}$$
$$=-\frac{1}{V_8}\left\{\mathbf{Q}^{(m)}V_8-\mathbf{Q}^nV_7+\frac{1}{2}\sum_{k=1}^{6}\left(\mathbf{Q}n_t+\mathbf{E}n_x+\mathbf{F}n_y+\mathbf{G}n_z\right)_k^{(m)}V_k\right.$$
$$\left.+\frac{1}{2}\sum_{k=1}^{6}\left(\mathbf{Q}n_t+\mathbf{E}n_x+\mathbf{F}n_y+\mathbf{G}n_z\right)_k^{n}V_k\right\}.$$

When $\Delta\mathbf{Q}^{(m)}$ on the left side of the equation converges to zero, the right-hand side becomes equal to zero and coincides with equation (1). That is to say, despite the numerical error which occurs by the inversion of matrix in left side of the equations and the linearization, time accuracy maintains second accuracy. These equations are solved in this work eventually. In this calculation, *m* times between the *n* step and the *n*+1 step are calculated until $\Delta\mathbf{Q}^{(m)}$ converges to some degree.

2.3 Discretization

The governing equations are three-dimensional Euler equations. The governing equations are discretized using Moving Grid FVM. Precision in space is second accuracy using the MUSCL approach. The convective numerical flux is calculated using SLAU and Roe upwind scheme. In time integration, the matrix-free LU-SGS implicit scheme is used with inner iteration method.

3. Steady problem

Before calculation of an unsteady problem, the code which is constructed based on Moving Grid FVM is validated by computing a steady problem. Calculation of the flow field around an ONERA M6 wing is done. In this calculation, the convective numerical flux is calculated using the SLAU upwind scheme. Figure 2 portrays the computational grid near the wing. A C–H type grid is created around the wing. The grid comprises 197 cells around the wing, 50 cells in a direction normal to the wing, and 82 cells in a spanwise direction. The computational domain is extended to 30 root chord lengths in a direction vertical to the wing. The smallest cell width is 5×10^{-3} root chord lengths. In flow conditions, the Mach number is 0.84 and the angle of attack is 3.06 deg. Figure 3(a) shows the pressure coefficient contours around the wing. The lambda shock, which is a feature of the ONERA M6 wing, can be confirmed. Figure 3(b) shows the pressure coefficient distribution of the wing section in 65 percent of semi span. As the figure shows, the computational results on the undersurface of the wing are well in agreement with experiment values. However, there is the difference near the shock wave on the upper surface of the wing. This results from inviscid calculation.

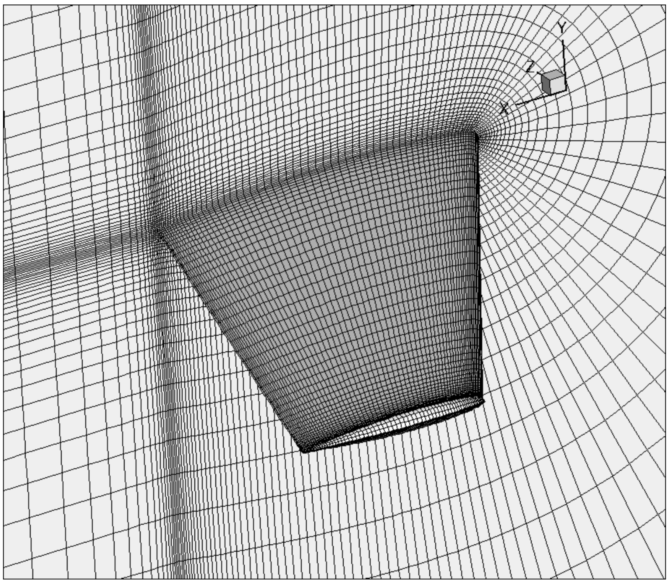

Fig. 2 Computational grid near the ONERA M6 wing.

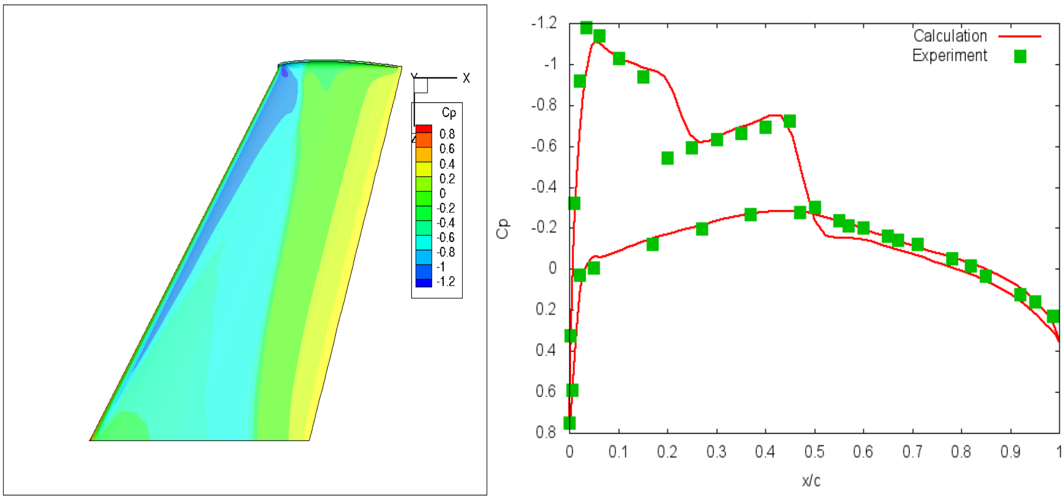

Fig. 3(a) Pressure coefficient contours of ONERA M6 wing and (b) pressure coefficient distribution of the wing section at a 65 semi span.

4. Unsteady problem

The pitching problem of NACA 0012 wing is then computed. In this calculation, the convective numerical flux is calculated using the Roe upwind scheme. Figure 4 shows the computational grid near the wing. This wing is an NACA 0012 airfoil extended in a z direction. This grid comprises 202 cells around the wing, 40 cells in a direction normal to the wing, and 10 cells in a z direction. The computational domain is extended 40 root chord lengths in a direction vertical to the wing. The smallest cell width is 10^{-3} root chord lengths. In this calculation, the pitching vibration is performed to the wing. The computational conditions accord with those from the experiment reported by Landon. The Mach number is 0.755. In vibration conditions, the mean angle of attack is

0.016 deg, the pitching amplitude is 2.51 deg, and the reduced frequency is 0.0814. The reduced frequency k is expressed as follows.

$$k = \frac{\omega c}{2V_\infty}.$$

In that equation, ω signifies frequency, c denotes chord length, and V_∞ represents the free stream velocity. Figure 5 shows the normal force coefficient distribution corresponding to the angle of attack. The red line shows computational results. The green points represent experimental values. The center point of this figure is a start point of vibration. Computational results draw the hysteresis loop with a pitching vibration. The trend of computational results agrees with this experimental one. However, the difference between computational results and experimental values arises, which results from ignoring viscosity. Therefore, for accurate computation, it is necessary to consider viscosity, which demands the use of Navier–Stokes equations.

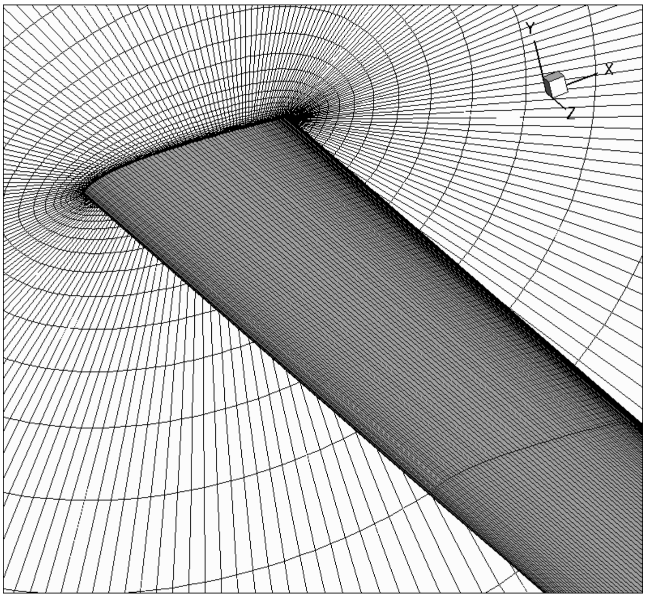

Fig. 4 Computational grid near NACA 0012 wing.

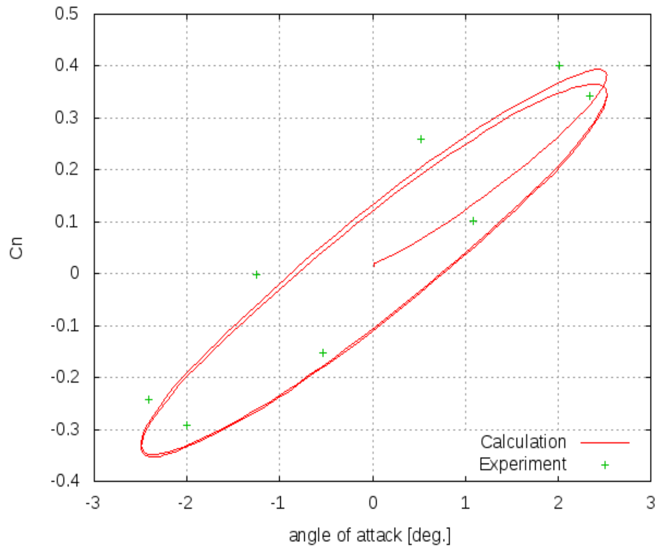

Fig. 5 Normal force coefficient distribution.

5. Conclusion

An unsteady flow calculation code is computed using Moving Grid FVM. First, Moving Grid FVM was formulated. Secondly, the flow field around ONERA M6 wing was computed. The computational results on the undersurface of the wing show good agreement with experimental values. However, there is the difference on the upper surface of the wing. Finally, the pitching problem of NACA 0012 wing was computed. The trend of computational results agrees with that of the experimental results. However, some gaps occurred between them. Viscosity must be considered to conduct computations accurately. As future works, Navier–Stokes equations will be considered, flutter simulations will be performed, and an unstructured grid will be applied to calculate the flow field around complicated objects.

References

[1] H. Im, X. Chen and G. Zha, “Prediction of a Supersonic Wing Flutter Boundary Using a High Fidelity Detached Eddy Simulation”, AIAA 2012-0039, 2012

[2] K. Mihara, K. Matsuno and N. Satofuka, “An Iterative Finite-Volume Scheme on a Moving Grid: First Report, The Fundamental Formulation and Validation”, Transactions of the Japan Society of Mechanical Engineers, Series B, Vol. 65, No. 637, 1999.